

Learning Graph-Based Geographical Latent Representation for Point-of-Interest Recommendation

Buru Chang
Korea University
buru_chang@korea.ac.kr

Seoyoon Kim
Korea University
sykim45@korea.ac.kr

Gwanghoon Jang
Korea University
simon0120@korea.ac.kr

Jaewoo Kang*
Korea University
kangj@korea.ac.kr

ABSTRACT

Several geographical latent representation models that capture geographical influences among points-of-interest (POIs) have been proposed. Although the models improve POI recommendation performance, they depend on shallow methods that cannot effectively capture highly non-linear geographical influences from complex user-POI networks. In this paper, we propose a new graph-based geographical latent representation model (GGLR) which can capture highly non-linear geographical influences from complex user-POI networks. Our proposed GGLR considers two types of geographical influences: *incoming influences* and *outgoing influences*. Based on a graph auto-encoder, geographical latent representations of incoming and outgoing influences are trained to increase geographical influences between two consecutive POIs that frequently appear in check-in histories. Furthermore, we propose a graph neural network-based POI recommendation model (GPR) that uses the trained geographical latent representations of incoming and outgoing influences for the estimation of user preferences. In the experimental evaluation on real-world datasets, we show that GGLR effectively captures highly non-linear geographical influences and GPR achieves state-of-the-art performance.

CCS CONCEPTS

• **Information systems** → **Collaborative filtering.**

KEYWORDS

Point-of-Interest; POI Recommendation; Recommender System; Location-based Social Network; Collaborative Filtering

ACM Reference Format:

Buru Chang, Gwanghoon Jang, Seoyoon Kim, and Jaewoo Kang. 2020. Learning Graph-Based Geographical Latent Representation for Point-of-Interest Recommendation. In *The 29th ACM International Conference on Information and Knowledge Management (CIKM '20), October 19–23, 2020, Virtual*

*Jaewoo Kang is the corresponding author.

Permission to make digital or hard copies of all or part of this work for personal or classroom use is granted without fee provided that copies are not made or distributed for profit or commercial advantage and that copies bear this notice and the full citation on the first page. Copyrights for components of this work owned by others than ACM must be honored. Abstracting with credit is permitted. To copy otherwise, or republish, to post on servers or to redistribute to lists, requires prior specific permission and/or a fee. Request permissions from permissions@acm.org.

CIKM '20, October 19–23, 2020, Virtual Event, Ireland

© 2020 Association for Computing Machinery.

ACM ISBN 978-1-4503-6859-9/20/10...\$15.00

<https://doi.org/10.1145/3340531.3411905>

Event, Ireland. ACM, New York, NY, USA, 10 pages. <https://doi.org/10.1145/3340531.3411905>

1 INTRODUCTION

In recent years, location-based social networks (LBSNs) such as Foursquare and Gowalla have grown in popularity. Users on LBSNs share their experiences and check-in information. Check-in histories generated by users are helpful for understanding user behavior patterns and preferences for points-of-interest (POIs). POI recommendation based on the check-in histories of users plays an important role in LBSNs. Since user behavior is limited by physical constraints, POI recommendation models should consider geographical influences among POIs to capture user behavior patterns and preferences for POIs, unlike conventional recommendation models used for tasks such as movie and product recommendation.

Several geographical latent representation models that capture geographical influences among POIs have been proposed. Existing geographical latent representation models can be grouped into two categories: explicit and implicit models. The following explicit models that use the geolocation information of POIs for training geographical latent representations have been proposed. USG [26], Rank-GeoFM [8], GeoSoCa [29], and STGCN [30] capture geographical influences using physical distances between POIs and various functions such as power-law and normal kernel functions. GeoMF [9] and IReNM [13] divide POIs into regions based on their geolocation, and train latent representations of the regions. Implicit or POI embedding models such as SG-CWARP [11] and CAPE [2] assume that POIs which co-occur in check-in histories are close to each other in distance. By considering such co-occurring POIs as neighbors, the models implicitly train geographical latent representations based on those of the neighbors. Furthermore, several geographical latent representation models that combine the above two approaches [3, 25, 31] have been recently proposed.

Although the aforementioned geographical latent representation models obtain improved POI recommendation performance, they depend on shallow methods (e.g., inner-product and dividing regions) to capture geographical influences among POIs. Figure 1 shows an example POI-POI network. The POI l_1 is influenced by not only the directly linked POIs l_2 , l_3 , and l_4 but also POIs that are not directly linked. However, some models [11, 20] that employ inner-product cannot effectively capture geographical influences among the POI l_1 and the indirectly linked POIs (l_5, l_6, \dots, l_9) [4]. Region-based models [9, 13] assume that POIs in the same region

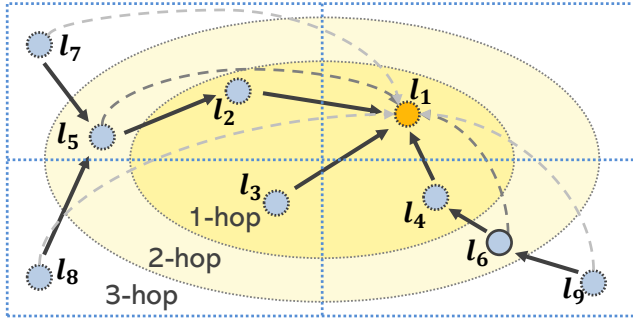


Figure 1: Complex POI-POI network. Rectangles indicate regions divided by geolocation information (latitude, longitude). The POI l_1 is influenced by not only the directly linked POIs l_2 , l_3 , and l_4 but also indirectly linked POIs.

have the same geographical influences. In the example, the region-based models regard the POIs l_3 and l_8 as having high geographical influences because the two POIs are in the same region. It causes a negative effect when the two POIs have a weak relationship (e.g., *Bar - Gym*). A previous study [19] found that the structure of complex networks is highly non-linear. Therefore, the shallow methods cannot capture highly non-linear geographical influences among POIs from complex user-POI networks [14, 20].

In this paper, we propose a new **Graph-based Geographical Latent Representation** model (GGLR) that captures highly non-linear geographical influences among POIs. As explained in [20, 24], geographical influences include *ingoing* and *outgoing* influences. Ingoing influence is defined as the influence of a POI on visitors from other POIs and outgoing influence is defined as the influence of a POI on its visitors to visit other POIs. For example, a *bar* that is usually the last stop of the day has higher ingoing influence from other POIs than outgoing influence to other POIs.

GGLR uses directed POI-POI graphs that reflect the ingoing and outgoing influences of POIs. Based on a graph auto-encoder [1], GGLR trains geographical latent representations of ingoing and outgoing influences to increase the geographical influences between two consecutive POIs that have a high visiting frequency. Graph neural networks (GNNs) [7], which are the core components of the graph auto-encoder, allow GGLR to capture latent representations of POIs from latent representations of their neighboring POIs. Therefore, GNNs are suitable for capturing highly non-linear geographical influences from complex POI-POI networks. Moreover, we use the physical distance between two POIs for learning geographical latent representations. Using the exponential function [20], we compute the physical distance feature. We apply the physical distance feature to the decoder of the graph auto-encoder. The distance feature makes geographical influences clear. For example, since a far-off airport and a hotel have a low physical distance feature value, the influence between the two POIs is increased if they frequently appear together in check-in histories.

Furthermore, we propose a **GNN-based POI Recommendation** (GPR) model that uses geographical latent representations trained by GGLR. We first construct a user-POI graph from user check-in histories. Based on higher-order GNNs [17], GPR extracts user

latent representations from trained geographical latent representations of outgoing influences of POIs visited by users. We then estimate user preferences for unvisited POIs based on the extracted user latent representations and trained geographical latent representations of ingoing influences of the POIs. Specifically, user preferences for POIs are estimated by multiplying the geographical latent representations of outgoing influences of POIs that users have visited by the geographical latent representations of ingoing influences of POIs that users have not yet visited. In the experimental evaluation on real-world LBSN datasets, we show that our proposed GPR model outperforms the existing baseline models.

The contributions of this paper are summarized as follows.

- We propose GGLR which is a new graph-based geographical latent representation model that captures highly non-linear geographical influences among POIs from complex user-POI networks. Based on the graph auto-encoder, our proposed GGLR trains geographical latent representations of ingoing and outgoing influences among POIs.
- We propose GPR which is a new GNN-based POI recommendation model that uses geographical latent representations of ingoing and outgoing influences trained by GGLR. Considering ingoing and outgoing influences, GPR extracts latent representations of users who have visited new POIs based on their visited POIs, and estimates user preferences for new POIs based on visited POIs.
- The experimental evaluation results on real-world LBSN datasets demonstrate that GPR achieves state-of-the-art performance.

The remainder of this paper is organized as follows. In Section 2, we summarize previously conducted researches related to our study. In Section 3, we describe our proposed GGLR and GPR. In Section 4, we compare GPR with existing POI recommendation models, and analyze the experimental results. Last, in Section 5, we provide the concluding remarks of our paper.

2 RELATED WORK

2.1 Geographical Latent Representation for POI Recommendation

The following geographical latent representation models that capture geographical influences among POIs from their geolocation information have been proposed. USG [26] and Rank-GeoFM [8] capture geographical influences based on the power-law distribution with physical distances. GeoMF [9] and iRenMF [13] divide POIs into regions based on the geolocation information of the POIs. Then, the models capture region-level geographical influences using matrix factorization (MF). GE [25] constructs a POI-region graph and a POI-POI graph to simultaneously use location-level and region-level geographical influences. Based on regions of POIs, POI2Vec [3] constructs a binary tree and applies a hierarchical softmax function to the binary tree to capture geographical influences. GeoSoCa [29] captures geographical influences based on a personalized distribution over latitude and longitude of POIs. Recently, the following adversarial learning algorithm-based geographical latent representation models have been proposed. Geo-ALM [10]

employs the adversarial learning algorithm for capturing region-level geographical influences. APOIR [32] considers neighboring POIs near users as positive labels. APOIR captures geographical influences while its discriminator classifies the POIs based on their labels.

The following Skip-Gram based [15] POI embedding models that capture geographical influences among POIs from check-in histories, which are considered as sequences of POIs, have been proposed. SG-CWARP [11] and Geo-Teaser [31] assume that POIs that co-occur in check-in histories are close to each in distance. The models train POI embedding vectors to increase geographical influences between co-occurring POIs. CAPE [2] is a content-aware POI embedding model that captures not only geographical influences but also characteristics of POIs from user-generated textual contents.

Our models are based on GeoIE [20] which considers the ingoing and outgoing influences. GeoIE adopts inner-product to train geographical latent representations of the influences and to estimate user preferences. In this paper, we propose GGLR and GPR both of which capture highly non-linear geographical latent representations of POIs from a complex user-POI graph.

2.2 Graph Neural Network-based Recommendation

With the success of GNN in representation learning, GNN-based recommendation models that have been proposed recently are as follows. sRMGCNN [16] uses GNNs to extract graph-based representations of users and items, and employs recurrent neural networks to estimate user preferences. GCMC [1] is a graph auto-encoder that trains latent representations of users and items from a user-item graph. PinSage [27] uses a randomwalk in GNN to learn latent representations of nodes in web-scale recommendation. NGCF [23] employs a high-order GNN that captures collaborative signals in representation learning.

GNN also has proven to be effective in capturing highly non-linear latent representations from heterogeneous information networks. RippleNet [21] utilizes a knowledge graph to incorporate side information of items. RippleNet considers not only directly linked neighboring items but also their k-hop neighboring items and side information. With attention mechanism, KGAT [22] computes the importance of relations in a knowledge graph.

Although GNNs are successful in capturing highly non-linear latent representations, they are not effective in learning geographical latent representations. To address this shortcoming, we propose a GNN-based geographical latent representation model that can learn geographical latent representations for POI recommendation.

3 OUR APPROACH

3.1 Preliminary

In this subsection, we define the data concepts and the POI recommendation task.

Definition 1 (User-POI graph) Let $\mathcal{U} = \{u_1, u_2, \dots, u_M\}$ and $\mathcal{L} = \{l_1, l_2, \dots, l_N\}$ denote a set of users and a set of POIs, respectively. We construct a bipartite user-POI graph $\mathcal{G}_r = (\mathcal{U}, \mathcal{L}, \mathcal{E}_r)$ where \mathcal{E}_r is the set of edges in the graph \mathcal{G}_r . The set of edges \mathcal{E}_r includes edge $e_{r,i,j}$ when a user u_i has visited POI l_j in the user's check-in

Table 1: Notations

Notation	Definition
$\mathcal{G}_r, \mathcal{G}_p$ \mathcal{U}, \mathcal{L}	User-POI graph, POI-POI graph Set of Users and POIs
\vec{p} \overleftarrow{q}	Latent representation of outgoing influence Latent representation of ingoing influence
$\vec{N}, \overleftarrow{N}$ $\vec{W}, \overleftarrow{W}$ $\vec{b}, \overleftarrow{b}$	Set of neighbors linked with outdegree and indegree Trainable weight matrices of GNN layers of GGLR Trainable bias terms of GNN layers of GGLR
W	Trainable weight matrix of decoder of GGLR
$e_{p,i,j}$ $\hat{e}_{p,i,j}$	Frequency of (POI $l_i \rightarrow$ POI l_j) in \mathcal{G}_p Estimated frequency of (POI $l_i \rightarrow$ POI l_j) by GGLR
$f(x_{i,j})$	Physical distance feature between POI l_i and POI l_j
u W_1, W_2 $r_{u,l}$	Latent representation of users Trainable weight matrices of GNN layers of GPR Estimated preference of user u for POI l

history.

Definition 2 (POI-POI graph) The check-in history of a user is a sequence of POIs the user visited. From a user's check-in history, we construct a directed POI-POI graph $\mathcal{G}_p = (\mathcal{L}, \mathcal{E}_p)$ where \mathcal{E}_p is the set of edges in the graph \mathcal{G}_p . An edge $e_{p,i,j}$ in the set of edges \mathcal{E}_p denotes the frequency of users consecutively visiting POI l_j after visiting POI l_i .

If there is a long time interval between two consecutive check-ins at POIs in the check-in history of a user, the correlation between the POIs is low [31]. Therefore, we count the frequency of $e_{p,i,j}$ when a user consecutively visits POI l_j after visiting POI l_i within h hours ($h \in \{3, 6, 12, 24, \infty\}$).

Definition 3 (POI recommendation) The POI recommendation task involves generating a list of ranked POIs that a user u is likely to visit next. The task in this study is defined with implicit feedback. Based on check-in histories, POI recommendation models estimate user preferences for unvisited POIs, and rank the POIs based on the estimated user preferences. The notations used in this paper are summarized in Table 1.

3.2 Graph-based Geographical Latent Representation Model

3.2.1 Geographical Latent Representation. As shown in Figure 1, the POI-POI network is complex. The shallow methods employed in many previous studies [20, 26, 28] could not effectively capture the highly non-linear geographical influences from the complex network. Thus, in this study, we employ GNN for effectively capturing highly non-linear geographical influences. GNN has proven to be effective in capturing non-linear latent representations from complex networks.

Based on the assumption that the more often users consecutively visit two POIs, the greater the geographical influence between the POIs, we propose a GGLR model that employs a graph auto-encoder [1]. There are ingoing and outgoing geographical influences among POIs. We utilize the directed POI-POI graph \mathcal{G}_p as the input of

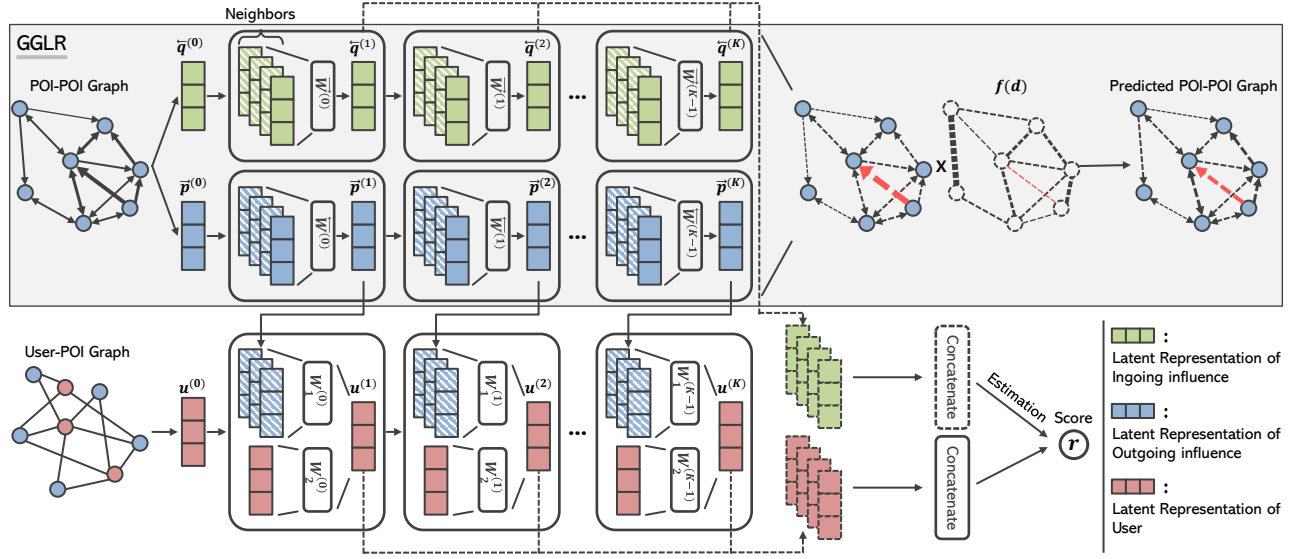


Figure 2: Architecture of GPR. Components in the gray box illustrate our proposed GGLR. Blue, green, and red color boxes denote the latent representations of outgoing influences, ingoing influences, and users, respectively. The patterned boxes denote latent representations of the neighboring nodes of each node in the POI-POI \mathcal{G}_p and user-POI \mathcal{G}_r graphs. In the POI-POI graph \mathcal{G}_p , edge thickness indicates the frequency of two consecutive POIs.

our GGLR because the graph reflects such ingoing and outgoing influences. For example, the frequency of (*restaurant* \rightarrow *bar*) is higher than the frequency of (*bar* \rightarrow *restaurant*).

The architecture of GGLR is illustrated in Figure 2. We use two structurally identical GNNs for ingoing and outgoing influences, respectively. Latent representations of outgoing influence $\vec{p}_i \in \mathbb{R}^d$ and those of ingoing influence $\vec{q}_i \in \mathbb{R}^d$ of a POI l_i of the k -th GNN layer ($1 \leq k \leq K$) are defined as follows:

$$\begin{aligned} \vec{p}_i^{(k)} &= \sigma\left(\frac{1}{|\vec{\mathcal{D}}_{(i)}|} \sum_{l_j \in \vec{\mathcal{N}}_{(i)}} e_{p,i,j} \times \vec{p}_j^{(k-1)} \vec{W}^{(k)} + \vec{b}^{(k)}\right), \\ \vec{q}_i^{(k)} &= \sigma\left(\frac{1}{|\vec{\mathcal{D}}_{(i)}|} \sum_{l_j \in \vec{\mathcal{N}}_{(i)}} e_{p,j,i} \times \vec{q}_j^{(k-1)} \vec{W}^{(k)} + \vec{b}^{(k)}\right), \end{aligned} \quad (1)$$

where $\sigma(\cdot)$ is the leaky version of the rectified linear unit (LeakyReLU). In the POI-POI graph \mathcal{G}_p , $\vec{\mathcal{N}}_{(i)}$ and $\vec{\mathcal{N}}_{(i)}$ denote the sets of neighboring POIs linked with $e_{p,i,j}$ and $e_{p,j,i}$, respectively. $\vec{W}^{(k)}, \vec{W}^{(k)} \in \mathbb{R}^{d \times d}$ and $\vec{b}^{(k)}, \vec{b}^{(k)} \in \mathbb{R}^d$ are the weight matrix and bias, respectively, of the k -th GNN layer. Since the graph \mathcal{G}_p is a directed graph, latent representations in Equation 1 are normalized by the sum of outdegrees and indegrees ($|\vec{\mathcal{D}}_{(i)}|$ and $|\vec{\mathcal{D}}_{(i)}|$). For each POI l_i in \mathcal{L} , we randomly initialize $\vec{p}_i^{(0)}$ and $\vec{q}_i^{(0)} \in \mathbb{R}^d$ with d -dimensional real-valued vectors and update them in the training phase.

Using the latent representations of outgoing $\vec{p}_i^{(K)}$ and ingoing $\vec{q}_j^{(K)}$ influences of K -th layer, we predict the frequency of consecutive POIs l_i and l_j as follows:

$$\hat{e}_{p,i,j} = (\vec{p}_i^{(K)} W) \cdot \vec{q}_j^{(K)}, \quad (2)$$

where $W \in \mathbb{R}^{d \times d}$ is the weight matrix of the bi-linear decoder of the graph auto-encoder, and $\hat{e}_{p,i,j}$ is the predicted frequency.

3.2.2 Physical Distance Feature. The physical distance between POIs is a significant factor that affects geographical influences. Therefore, many POI recommendation models use physical distance information to rank POIs, and highly rank POIs near visited POIs. However, this might lead to performance degradation. For example, even though a *bar* and a *brunch restaurant* are in the same building, users are not likely to visit the *brunch restaurant* after visiting the *bar* at night. On the other hand, users are likely to visit an *accommodation* after arriving at an *international airport* even though the *accommodation* is far from the *airport*. To address this issue, we use physical distance information for learning geographical latent representations, not for estimating user preferences.

We first compute the physical distance feature using the exponential function [20]. The exponential function computes the physical distance feature as high when two POIs are close to each other while it computes the physical distance feature as low when the two POIs are far apart. The physical distance $x_{i,j}$ between the POI l_i and POI l_j is expressed in kilometers and clamped in the range $[0.01\text{km}, 100\text{km}]$. Physical distances that are farther than 100 km are treated as 100 km. Given physical distance $x_{i,j}$, the exponential function is defined as follows:

$$f(x_{i,j}) = a * x_{i,j}^b * e^{cx_{i,j}}, \quad (3)$$

where a , b , and c are trainable variables. We then modify Equation 2 with the exponential function as follows:

$$\hat{e}_{p,i,j} = f(x_{i,j}) \times (\vec{p}_i^{(K)} W) \cdot \vec{q}_j^{(K)}. \quad (4)$$

The physical distance feature plays a role that makes the geographical influence clear. The red lines in Figure 2 show the following

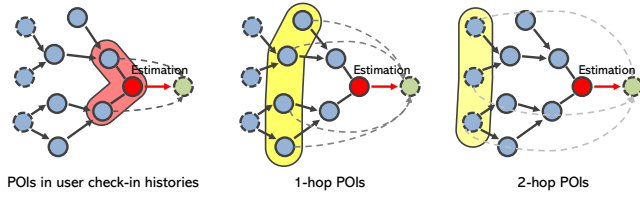


Figure 3: Motivation for the structure of GPR.

scenario. The POIs *airport* and *accommodation* are far from each other, but the frequency of (*airport* \rightarrow *accommodation*) is high. Since the physical distance feature $f(x_{i,j})$ between the *airport* and *accommodation* is low, the geographical influence $(\vec{p}_i^{(K)} W) \cdot \vec{q}_j^{(K)})$ computed by multiplying the geographical latent representation of the outgoing influence of the *airport* and the geographical latent representation of the ingoing influence of the *accommodation* is increased.

All the trainable parameters of GGLR are optimized by minimizing the following loss function defined with the mean square error:

$$\mathcal{L}_p(\theta_p) = \frac{1}{|\mathcal{E}_p|} \sum_{e_p} (e_p - \hat{e}_p)^2, \quad (5)$$

where θ_p is the set of trainable parameters of GGLR.

3.3 Graph Neural Network-based Point-of-Interest Recommendation Model

3.3.1 User Latent Representation. The POI recommendation task involves recommending POIs that users are likely to visit based on their check-in histories. In Figure 3, the red node and red box denote a user u and the user's check-in histories, respectively. The blue nodes in the red box denote the POIs l_u visited by the user u . The blue nodes in the yellow boxes denote the n -hop neighboring POIs l'_u of the POIs l_u in the POI-POI graph \mathcal{G}_p . To estimate the preference of the user u for a target POI (green node), we should consider the geographical influences between the target POI and the POIs l_u in the user u 's check-in history. In addition, since the n -hop neighbor POIs l'_u can influence the target POI, we also have to consider the geographical influences of the POIs l'_u .

To do this, we propose GPR which extends a higher-order GNN [17] with GGLR. Figure 2 shows the architecture of our GPR model. Each layer of the higher-order GNN is computed as follows:

$$f^{(k)}(v) = \sigma(f^{(k-1)}(v)W_1^{(k)} + \sum_{w \in \mathcal{N}(v)} f^{(k-1)}(w)W_2^{(k)} + b^{(k)}), \quad (6)$$

where $f^{(k)}(v) \in \mathbb{R}^d$ is the latent representation of the node v of the k -th layer. The higher-order GNN uses different weight matrices (W_1 and $W_2 \in \mathbb{R}^{d \times d}$) for the node v and its neighbors w , which is the distinct feature of the higher-order GNN. We exploit this feature to extract the latent representations of users from the bipartite user-POI graph \mathcal{G}_r . Using the outgoing influences \vec{p}_j of POIs trained by GGLR, we modify Equation 6 to capture the latent representation u_i of the user u_i as follows:

$$u_i^{(k)} = \sigma(u_i^{(k-1)}W_1^{(k)} + \sum_{l_j \in \mathcal{N}(i)} \vec{p}_j^{(k)}W_2^{(k)} + b^{(k)}), \quad (7)$$

where $\mathcal{N}(i)$ is the set of POIs linked with the user u_i in the user-POI graph \mathcal{G}_r . $b \in \mathbb{R}^d$ is the bias of the k -th GNN layer.

Like the gray dashed arrows in Figure 3, we assume that the user u is starting from each POI in their check-in history. Thus, GPR uses geographical latent representations of outgoing influences as latent representations of POIs. Moreover, based on GGLR, GPR can consider the n -hop neighbor POIs l'_u that influence the target POI but are not directly linked to the target POI. W_1 and W_2 are trained for latent representations of users u and outgoing influences \vec{p} of POIs, respectively. This makes it possible to consider and to preserve the characteristics of the user and POI nodes of the bipartite graph when aggregating latent representations of each GNN layer. We randomly initialize $u^{(0)} \in \mathbb{R}^d$ for each user u , and use it as the input of the first GNN layer.

The main difference between GPR and the higher-order GNN is that the higher-order GNN models the latent representations of users and POIs at the same time, while GPR models only latent representations of users. Employing GGLR's outgoing influences as latent representations of POIs, GPR can consider significantly more POIs that geographically influence the target POI.

3.3.2 User Preference Estimation. We then estimate user preferences for POIs using the extracted user latent representations u and geographical latent representations of ingoing influences \vec{q} . Through K' GNN layers, we obtain K' user latent representations for each user. Since the user latent representations u of each GNN layer are captured from the geographical latent representations \vec{p} of outgoing influences of the corresponding layer, they cover different levels of multi-hop neighbor POIs. Thus, we concatenate all the user latent representations for the estimation of user preferences, and use it as the final user latent representations. In the same manner, we concatenate all the geographical latent representations of the ingoing influences, which are trained by different GGLR layers. The user preferences are estimated as follows:

$$u = [u^1; u^2; \dots; u^{K'}], \quad \vec{q} = [\vec{q}^1; \vec{q}^2; \dots; \vec{q}^{K'}], \quad (8)$$

$$r_{u,l} = u^T \vec{q}_l, \quad (9)$$

where $r_{u,l}$ is the estimated preference of a user u for a POI l , and K' ($1 \leq K' \leq K$) is the number of higher order GNN layers. For estimating a user's preferences for POIs, the user is represented with the outgoing influence of POIs that the user has visited, and multiplying it by the ingoing influences of POIs that the user has not yet visited. We emphasize that our estimated user preferences reflect the outgoing influences and ingoing influences of POIs.

3.3.3 Optimization. To optimize the parameters θ_r used for the estimation of user preferences, we use a pairwise ranking-based loss function [18] to consider the relative preferences between visited and unvisited POIs. We assume that user preferences for visited POIs are relatively higher than preferences for unvisited POIs. The loss function is defined as follows:

$$\mathcal{L}_r(\theta_r) = \sum_{(u,l,l') \in \mathcal{O}} -\log(\hat{\sigma}(r_{u,l} - r_{u,l'})), \quad (10)$$

where $\mathcal{O} = \{(u,l,l') | e_{r,u,l} \in \mathcal{E}_r, e_{r,u,l'} \notin \mathcal{E}_r\}$ denotes the training data constructed from visited POIs l and randomly sampled unvisited POIs l' . $\hat{\sigma}$ is the sigmoid function.

Table 2: Statistics of the datasets.

Statistics	Gowalla	Foursquare	Yelp
# of Check-ins	1,278,274	1,196,248	860,888
# of POIs	32,510	28,593	18,995
# of Users	18,737	24,941	30,887
Avg. # of Check-ins per User	68.22	41.84	27.87
Avg. # of POIs per User	43.87	28.75	26.58
Avg. # of Users per POI	25.28	25.08	43.21
Sparsity	99.865%	99.900%	99.860%

The final loss function $\mathcal{L}(\theta)$ of our GPR proposed in this study consists of the loss functions $\mathcal{L}_r(\theta_r)$ and $\mathcal{L}_p(\theta_p)$:

$$\mathcal{L}(\theta) = \mathcal{L}_r(\theta_r) + \lambda_1 \mathcal{L}_p(\theta_p) + \lambda_2 (\|\theta_r\|_2^2 + \|\theta_p\|_2^2), \quad (11)$$

where the third term denotes L_2 -regularization used for preventing overfitting. The hyperparameters λ_1 and λ_2 control the effect of GGLR and the L_2 -regularization, respectively. Using the Adam optimizer [6], all the trainable parameters θ of GPR including θ_r and θ_p are optimized by minimizing the loss function $\mathcal{L}(\theta)$ in the training phase.

4 EXPERIMENTAL EVALUATION

4.1 Evaluation Setup

4.1.1 Datasets. Our experimental evaluation was conducted on the following three public LBSN datasets. We obtained the datasets from Liu et al. [12] who processed the datasets.

The statistics of the datasets are summarized in Table 2.

(1) Gowalla: The Gowalla dataset¹ contains check-in histories generated on Gowalla from February 2009 to October 2010. Users who visited fewer than 15 POIs and POIs with fewer than 10 visitors were removed. After preprocessing, the Gowalla dataset contains 1,278,274 check-ins by 18,737 users and 32,510 POIs.

(2) Foursquare The Foursquare dataset includes check-in histories generated on Foursquare from April 2012 to September 2013. As done for the Gowalla dataset, users who visited fewer than 10 POIs and POIs visited by fewer than 10 users were removed. The preprocessed Foursquare dataset includes 1,196,248 check-ins by 24,941 users and 28,593 POIs.

(3) Yelp The Yelp dataset² contains check-in histories generated on Yelp. Users who visited fewer than 10 POIs and POIs with fewer than 10 visitors were removed. The final Yelp dataset consists of 860,888 check-ins by 30,887 users and 18,995 POIs.

Each dataset was divided into training, validation, and test sets. 70% of the check-ins (oldest) and 20% of the check-ins (more recent) of users were used as the training and test sets, respectively. The remaining 10% of the check-ins (newest) were used as the validation set.

4.1.2 Baselines. In many research studies on POI recommendation, auxiliary information such as social relationships [29] and temporal information [10, 28, 33] are used for improving POI recommendation performance. However, in this paper, we focus on

only geographical influences among POIs for POI recommendation. Therefore, for a fair comparison, we compare our proposed GPR with the following baseline models that also focus only on geographical influences among POIs:

(1) IRenMF: IRenMF [13] is based on weighted MF [5]. IRenMF simultaneously considers location-level and region-level geographical influences.

(2) GeoMF: GeoMF [9] is a weighted MF model that uses region-level geographical influences.

(3) Rank-GeoFM: Rank-GeoFM [8] is a ranking-based matrix factorization model that learns user preferences for POIs based on trained geographical influences among neighboring POIs.

(4) Geo-Teaser: Based on Skip-Gram [15], Geo-Teaser [31] captures geographical influences from check-in histories. Geo-Teaser captures relative user preferences for POIs based on geographical influences.

(5) GeoIE: GeoIE [20] considers outgoing and ingoing geographical influences. GeoIE employs the inner-product to capture geographical influences from geographical latent representations of outgoing and ingoing influences.

(6) APOIR: APOIR [32] learns the underlying user preferences for POIs in an adversarial manner. Since APOIR leverages temporal information, we replace its temporal GRU with MF-based user latent representations for a fair comparison.

We exclude several state-of-the-art POI recommendation models such as TEMN [33] and STGN [30], which utilize POI sequences as inputs for recommending the next POI, since they are designed for successive POI recommendation.

4.1.3 Evaluation Metrics. To assess the performance of the recommendation models, we use the following four widely-used evaluation metrics: **precision@n**, **recall@n**, mean average precision (**MAP@n**), and normalized discounted cumulative gain (**NDCG@n**) where n is the number of POIs in the ranked list. Precision@ n and Recall@ n scores are high when the correct POI is in the top- n POIs. MAP@ n and NDCG@ n are used to measure the quality of the list of ranked POIs. When the correct POI is ranked high in the recommendation list, the evaluation score is high. In this experimental evaluation, we report the evaluation results for $n = 5, 10, 20$, and 50.

4.1.4 Details. We obtained the source code for IRenMF, GeoMF, and RankGeoFM from Liu et al. [12] and evaluated the models. We also obtained the source code for APOIR made available by its authors and evaluated the model. We implemented the deep learning-based models Geo-Teaser, GeoIE, and GPR using PyTorch library v1.4. Using the validation set, we searched for the optimal hyperparameters for each model by maximizing recall@10. The dimension of latent representations was searched in {8, 16, 32, 64, 128}. The dropout rate was searched in {0.1, 0.2, 0.3, 0.4, 0.5, 0.6, 0.7}. The parameter λ_2 for the L_2 -regularization was searched in {0.00001, 0.00005, 0.0001, 0.0005, 0.001, 0.005, 0.01}. The learning rate of each model was searched in {0.0001, 0.0005, 0.001, 0.005, 0.01}. For our proposed GPR, the parameter λ_1 that controls the effect of GGLR was searched in {0.1, 0.2, 0.3, 0.4, 0.5}. The time interval h for construction of the POI-POI graph \mathcal{G}_p was searched in {3, 6, 12, 24, ∞ }. The numbers of GNN layers K were searched in the range [1,

¹<http://snap.stanford.edu/data/loc-gowalla.html>

²Yelp Dataset Challenge Round 7 (access date: Feb 2016), <https://www.yelp.com/dataset/challenge>

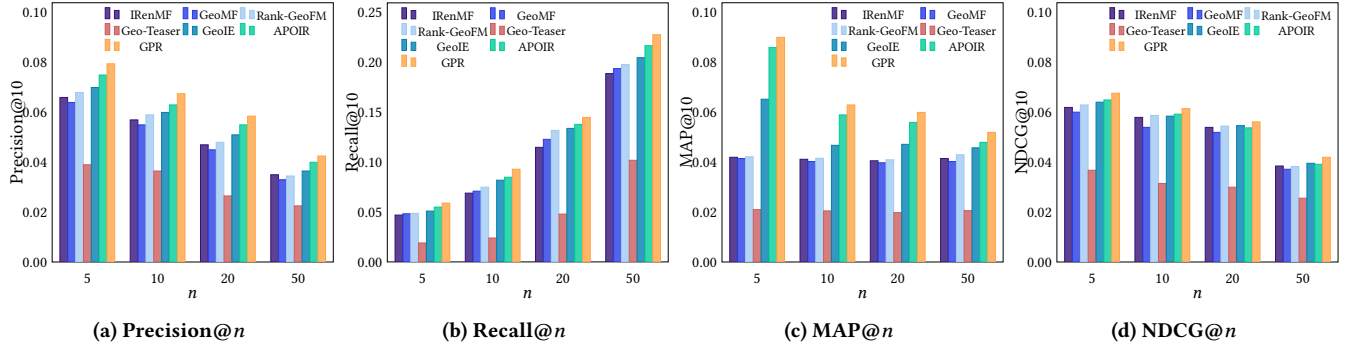


Figure 4: Performance comparison of GPR and the baselines on the Gowalla dataset as n increases.

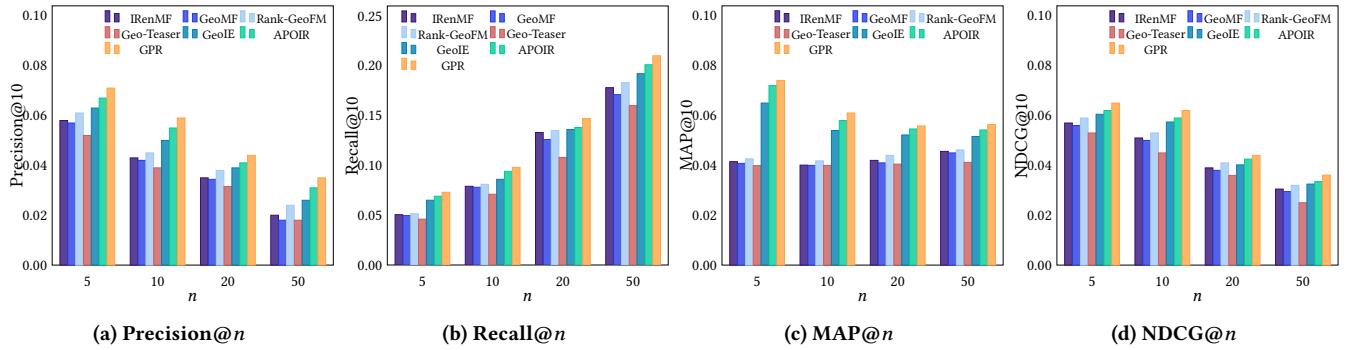


Figure 5: Performance comparison of GPR and the baselines on the Foursquare dataset as n increases.

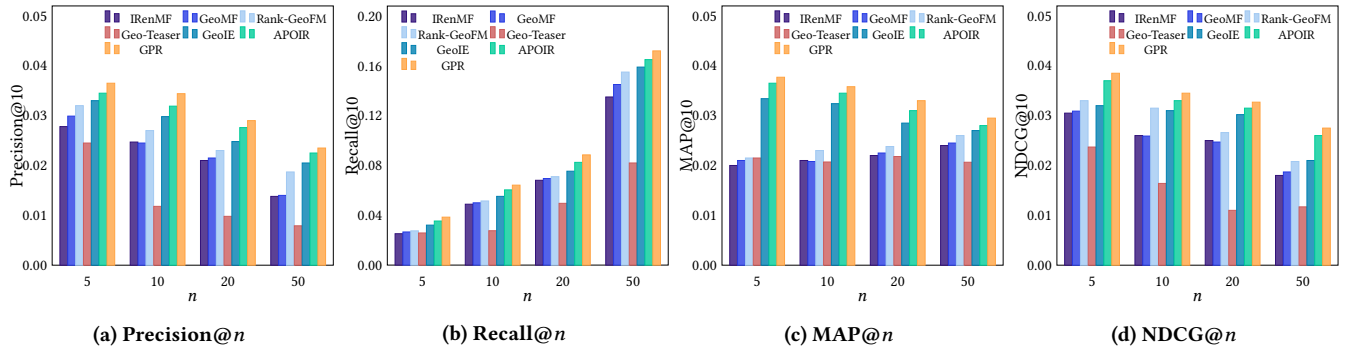


Figure 6: Performance comparison with the baselines on the Yelp dataset as n increases.

4]. The optimal hyperparameters of the proposed GPR model are described in the 4.2.3 subsection.

4.2 Evaluation Results

4.2.1 Performance Comparison. The evaluation results on the three LBSN datasets are summarized in Figures 4, 5, and 6, respectively. The results show that our GPR outperformed all the baselines on the three datasets. In detail, on the Gowalla dataset, the GPR model obtained 7.1%-84.9%, 9.4%-287.5%, 6.8%-207.3%, and 3.7%-95.2% improvements over all the baselines in Precision@10, Recall@10, MAP@10, and NDCG@10, respectively. On the Foursquare dataset,

GPR obtained 7.3%-51.3%, 4.3%-38.0%, 5.2%-52.5%, and 5.1%-37.8% improvements over all the baselines in Precision@10, Recall@10, MAP@10, and NDCG@10, respectively. Last, GPR obtained 7.8%-191.5%, 3.8%-132.6%, 6.3%-72.9%, and 4.5%-110.3% improvements over all the baselines in Precision@10, Recall@10, MAP@10, and NDCG@10, respectively, on the Yelp dataset. Notably, GPR outperformed GeoIE which also considers ingoing and outgoing geographical influences. This result demonstrates that our GNN-based GGLR and GPR models more effectively capture highly non-linear geographical influences and user preferences for POIs, respectively,

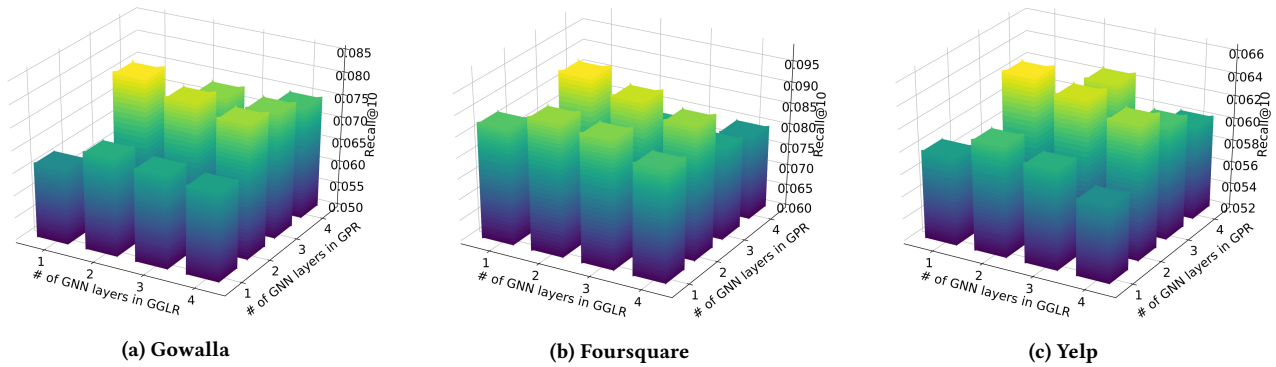


Figure 7: Effect of the number of GNN layers K and K' in GGLR and GPR, respectively.

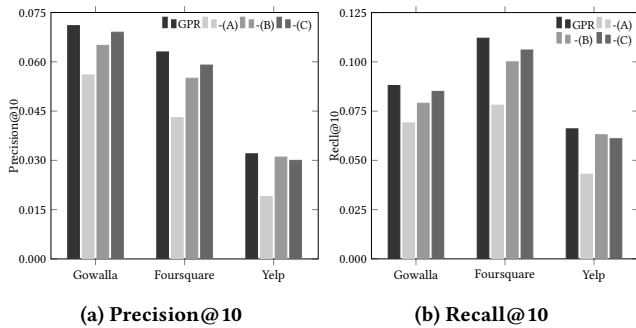


Figure 8: Ablation test results on the three datasets. -(A), -(B), and -(C) denote the removed components GGLR, asymmetric features, and physical distance features, respectively.

than GeoIE which employs the shallow method to capture geographical influences and user preferences.

We also conducted one-sample t-tests over the strongest baseline model to measure the statistical significance of improvements of our proposed GPR. For all the three datasets, we obtained p-values less than 0.05, which indicates that the improvements of GPR over the strongest baseline are statistically significant.

4.2.2 Effectiveness of Each Component. To assess the effectiveness of each component of the GPR, we conducted an ablation test. Figure 8 presents the results of the ablation test on the three datasets, where changes in performance are reported after each component is removed at a time. We individually removed the following components and observed for changes in Precision@10 and Recall@10. **(A) GGLR:** We removed $\mathcal{L}_p(\theta_p)$ from Equation 11 to verify the effectiveness of GGLR. Geographical latent representations and user latent representations are randomly initialized and updated in an MF manner.

The performance decreased considerably when we removed GGLR, which demonstrates that GGLR contributes to improving performance by capturing highly non-linear geographical influences among POIs. The effectiveness of GGLR on the Foursquare and Yelp datasets, both of which contain a smaller number of check-ins per user than Gowalla, is greater than on the Gowalla dataset.

These results show that geographical influences captured by GGLR are more useful when check-in histories are insufficient for capturing user preferences for POIs.

(B) ingoing and outgoing geographical influences: We did not consider ingoing and outgoing geographical influences. We used latent representations of outgoing influences \vec{p} instead of latent representations of ingoing influences \vec{q} in Equations 1 and 7.

Also, the performance on the Gowalla and Foursquare datasets decreased when we did not consider the ingoing and outgoing geographical influences of POIs. This result demonstrates that there exist ingoing and outgoing geographical influences, and GGLR effectively captures ingoing and outgoing influences from the directed POI-POI graph. Thus, the structure of GPR, which uses outgoing influences for user latent representations and estimates user preferences based on ingoing influences, is effective. GPR obtains improved performance by utilizing them for estimating user preferences. However, the ingoing and outgoing geographical influences did not help improve performance much on the Yelp dataset, unlike on the Gowalla and Foursquare datasets. Since Yelp is a review forum for POIs rather than LBSNs, the successiveness of two consecutive check-ins in the Yelp dataset is lower than on other datasets. Therefore, capturing asymmetric features from the directed POI-POI graph constructed from consecutive check-ins in the Yelp dataset is difficult.

(C) Physical distance feature: We removed the physical distance feature $f(x)$ from Equation 4 to verify the effectiveness of the physical distance feature.

The performance of GPR degraded when we removed the physical distance features. Many previous studies use physical distance features for the estimation of user preferences to improve performance. On the other hand, GGLR utilizes the physical distance features to make effective latent representations of geographical influences, which contribute to improving performance.

4.2.3 Hyperparameter Optimization. We observed performance variance when we changed the hyperparameters of GPR. We report the performance in terms of Recall@10.

Figure 7 shows the variations in Recall@10 when we change the number of GNN layers K and K' in GGLR and GPR, respectively. K' is less than or equal to K because each layer of GPR depends on

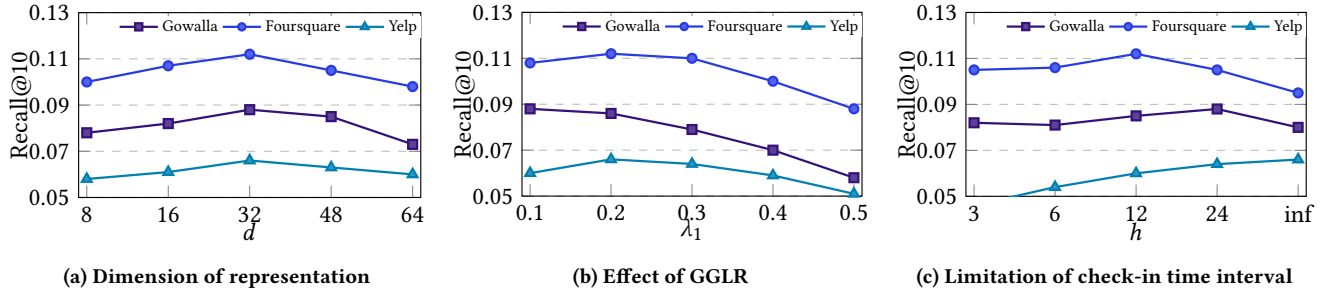


Figure 9: Effects of hyperparameters.

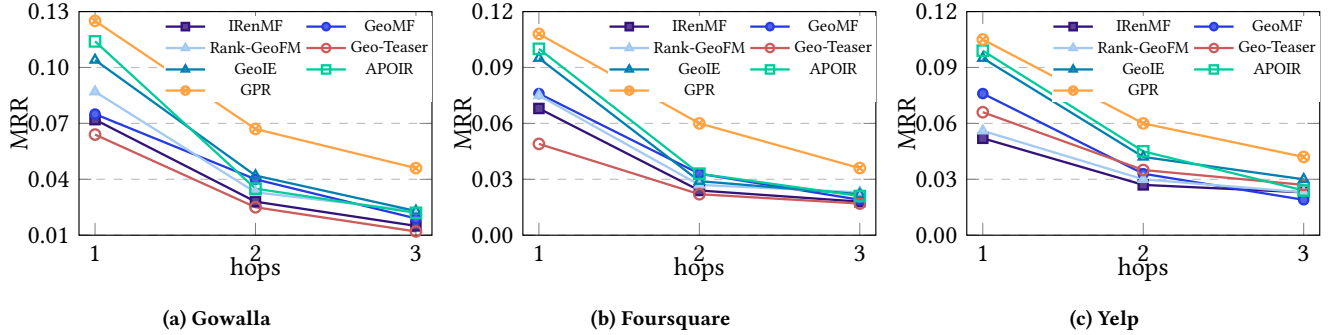


Figure 10: Performance evaluation results depending on the level of hops.

geographical latent representations of outgoing influences, trained in each GGLR layer. The best performance on all the datasets was obtained when K and K' were set to 2. The results demonstrate that the two GNN layers (2-hops) are sufficient for capturing geographical influences and user behavior patterns from POIs' and users' neighbors, respectively.

As shown in Figure 9a, the best performance on all the datasets is obtained when the dimension d of latent representations is set to 32. The hyperparameter λ_1 controls the effect of GGLP in the parameter optimization. The performance variance due to the hyperparameter is summarized in Figure 9b. The best performance on the Foursquare and Yelp datasets was obtained when we used $\lambda_1=0.2$. The best performance on the Gowalla dataset was obtained when $\lambda_1=0.1$ was used. As described in the subsection 4.2.2, GGLR is more effective when the number of check-ins of users is insufficient for capturing user preferences for POIs. Therefore, the performance of GGLR on the Foursquare and Yelp datasets is higher than that on the Gowalla dataset.

Several previous studies [11, 31] show that the time interval between two consecutive check-ins at POIs affects the geographical influences between the POIs. For example, consecutive check-ins on different days may not be highly correlated. As shown in Figure 9c, we obtained the best performance on the Gowalla and Foursquare datasets when we constructed the POI-POI graph from consecutive check-ins within 24 hours and 12 hours, respectively. Interestingly, we obtained the best performance on the Yelp dataset when we constructed the POI-POI graph \mathcal{G}_p without considering time interval h . Since most time intervals between two consecutive check-ins in

the Yelp dataset are longer than 24 hours, the POI-POI graph is too sparse to capture geographical influences when h is shorter than 24 hours. Therefore, we should not consider time intervals between check-ins when constructing the POI-POI graph \mathcal{G}_p for the Yelp dataset.

4.2.4 Non-linearity of Geographical Influences. In this subsection, we aim to verify that geographical influences captured by GGLR are more non-linear than geographical influences captured by other models. In the directed POI-POI graph \mathcal{G}_p , we first searched for the shortest path between a visited POI and a POI of the test data. We then grouped test data corresponding to the number of hops in the shortest path. For example, the relation between the POI l_1 and the POI l_3 in the shortest path ($l_1 \rightarrow \hat{l}_2 \rightarrow l_3$) is 2-hop where l_1 is the visited POI in the training data, \hat{l}_2 is the unvisited POI, and l_3 is the POI in test data. The mean reciprocal rank (MRR) scores on each group were computed.

Figure 10 shows the MRR scores obtained on the three datasets. MRR scores are high when the correct POIs are ranked high in the recommended POI list. As shown in the figure, for all the levels of hops, GPR outperformed all the baseline models. GPR achieved relatively high MRR scores on 2-hop and 3-hop than the baseline models. The results demonstrate that GPR more accurately estimates user preferences for POIs that have weak links with visited POIs. GPR captures geographical influences using GGLR which considers not only directly linked POIs but also multiple-hop neighboring POIs. These results show that GGLR captures the more highly nonlinear geographical influences from the complex user-POI network than the baseline models which employ shallow methods.

5 CONCLUSION AND FUTURE WORK

In this paper, we proposed a graph-based geographical latent representation model called GGLR. GGLR captures ingoing and outgoing geographical influences from the directed POI-POI graph constructed from check-in histories. GGLR also uses physical distance features to make more effective geographical latent representations. We also proposed GPR which is a graph-based POI recommendation model. Utilizing GGLR, GPR extracts user latent representations from geographical latent representations of outgoing influences of POIs. GPR then estimates the user preferences for POIs based on the extracted user latent representations and geographical latent representations of ingoing influences of POIs. We showed that our proposed GPR outperforms the state-of-the-art POI recommendation models. Last, the experimental evaluation results demonstrate that our proposed GGLR model effectively captures highly non-linear geographical influences and GPR achieves better performance utilizing the geographical influences captured by GGLR.

For future work, we plan to apply GGLR to the successive POI recommendation task in which user check-in sequences are used as input. We will also address cold-start problems, which are not addressed in this paper, in future work.

ACKNOWLEDGEMENTS

This research was supported by the National Research Foundation of Korea (No. NRF-2017R1A2A1A17069645, NRF-2017M3C4A7065887).

REFERENCES

- [1] Rianne van den Berg, Thomas N Kipf, and Max Welling. 2017. Graph convolutional matrix completion. *arXiv preprint arXiv:1706.02263* (2017).
- [2] Buru Chang, Yonggyu Park, Donghyeon Park, Seongsoo Kim, and Jaewoo Kang. 2018. Content-Aware Hierarchical Point-of-Interest Embedding Model for Successive POI Recommendation. In *IJCAI*. 3301–3307.
- [3] Shanshan Feng, Gao Cong, Bo An, and Yeow Meng Chee. 2017. Poi2vec: Geographical latent representation for predicting future visitors. In *Thirty-First AAAI Conference on Artificial Intelligence*.
- [4] Xiangnan He, Lizi Liao, Hanwang Zhang, Liqiang Nie, Xia Hu, and Tat-Seng Chua. 2017. Neural collaborative filtering. In *Proceedings of the 26th International Conference on World Wide Web*. International World Wide Web Conferences Steering Committee, 173–182.
- [5] Yifan Hu, Yehuda Koren, and Chris Volinsky. 2008. Collaborative filtering for implicit feedback datasets. In *2008 Eighth IEEE International Conference on Data Mining*. Ieee, 263–272.
- [6] Diederik P Kingma and Jimmy Ba. 2014. Adam: A method for stochastic optimization. *arXiv preprint arXiv:1412.6980* (2014).
- [7] Thomas N Kipf and Max Welling. 2016. Semi-supervised classification with graph convolutional networks. *arXiv preprint arXiv:1609.02907* (2016).
- [8] Xutao Li, Gao Cong, Xiao-Li Li, Tuan-Anh Nguyen Pham, and Shonali Krishnaswamy. 2015. Rank-geofm: A ranking based geographical factorization method for point of interest recommendation. In *Proceedings of the 38th International ACM SIGIR Conference on Research and Development in Information Retrieval*. ACM, 433–442.
- [9] Defu Lian, Cong Zhao, Xing Xie, Guangzhong Sun, Enhong Chen, and Yong Rui. 2014. GeoMF: joint geographical modeling and matrix factorization for point-of-interest recommendation. In *Proceedings of the 20th ACM SIGKDD international conference on Knowledge discovery and data mining*. ACM, 831–840.
- [10] Wei Liu, Zhi-Jie Wang, Bin Yao, and Jian Yin. 2019. Geo-ALM: POI recommendation by fusing geographical information and adversarial learning mechanism. In *Proceedings of the 28th International Joint Conference on Artificial Intelligence*. AAAI Press, 1807–1813.
- [11] Xin Liu, Yong Liu, and Xiaoli Li. 2016. Exploring the Context of Locations for Personalized Location Recommendations. In *IJCAI*. 1188–1194.
- [12] Yiding Liu, Tuan-Anh Nguyen Pham, Gao Cong, and Quan Yuan. 2017. An experimental evaluation of point-of-interest recommendation in location-based social networks. *Proceedings of the VLDB Endowment* 10, 10 (2017), 1010–1021.
- [13] Yong Liu, Wei Wei, Aixin Sun, and Chunyan Miao. 2014. Exploiting geographical neighborhood characteristics for location recommendation. In *Proceedings of the 23rd ACM International Conference on Conference on Information and Knowledge Management*. ACM, 739–748.
- [14] Jarana Manotumruksa, Craig Macdonald, and Iadh Ounis. 2017. A deep recurrent collaborative filtering framework for venue recommendation. In *Proceedings of the 2017 ACM on Conference on Information and Knowledge Management*. ACM, 1429–1438.
- [15] Tomas Mikolov, Ilya Sutskever, Kai Chen, Greg S Corrado, and Jeff Dean. 2013. Distributed representations of words and phrases and their compositionality. In *Advances in neural information processing systems*. 3111–3119.
- [16] Federico Monti, Michael Bronstein, and Xavier Bresson. 2017. Geometric matrix completion with recurrent multi-graph neural networks. In *Advances in Neural Information Processing Systems*. 3697–3707.
- [17] Christopher Morris, Martin Ritzert, Matthias Fey, William L Hamilton, Jan Eric Lenssen, Gaurav Rattan, and Martin Grohe. 2019. Weisfeiler and leman go neural: Higher-order graph neural networks. In *Proceedings of the AAAI Conference on Artificial Intelligence*, Vol. 33. 4602–4609.
- [18] Steffen Rendle, Christoph Freudenthaler, Zeno Gantner, and Lars Schmidt-Thieme. 2012. BPR: Bayesian personalized ranking from implicit feedback. *arXiv preprint arXiv:1205.2618* (2012).
- [19] Daixin Wang, Peng Cui, and Wenwu Zhu. 2016. Structural deep network embedding. In *Proceedings of the 22nd ACM SIGKDD international conference on Knowledge discovery and data mining*. ACM, 1225–1234.
- [20] Hao Wang, Huawei Shen, Wentao Ouyang, and Xueqi Cheng. 2018. Exploiting POI-Specific Geographical Influence for Point-of-Interest Recommendation. In *IJCAI*. 3877–3883.
- [21] Hongwei Wang, Fuzheng Zhang, Jialin Wang, Miao Zhao, Wenjie Li, Xing Xie, and Minyi Guo. 2018. Ripplenet: Propagating user preferences on the knowledge graph for recommender systems. In *Proceedings of the 27th ACM International Conference on Information and Knowledge Management*. 417–426.
- [22] Xiang Wang, Xiangnan He, Yixin Cao, Meng Liu, and Tat-Seng Chua. 2019. Kgat: Knowledge graph attention network for recommendation. In *Proceedings of the 25th ACM SIGKDD International Conference on Knowledge Discovery & Data Mining*. 950–958.
- [23] Xiang Wang, Xiangnan He, Meng Wang, Fuli Feng, and Tat-Seng Chua. 2019. Neural graph collaborative filtering. In *Proceedings of the 42nd international ACM SIGIR conference on Research and development in Information Retrieval*. 165–174.
- [24] Yongqing Wang, Huawei Shen, Shenghua Liu, and Xueqi Cheng. 2015. Learning user-specific latent influence and susceptibility from information cascades. In *Proceedings of the Twenty-Ninth AAAI Conference on Artificial Intelligence*. AAAI Press, 477–483.
- [25] Min Xie, Hongzhi Yin, Hao Wang, Fanjiang Xu, Weitong Chen, and Sen Wang. 2016. Learning graph-based poi embedding for location-based recommendation. In *Proceedings of the 25th ACM International on Conference on Information and Knowledge Management*. ACM, 15–24.
- [26] Mao Ye, Peifeng Yin, Wang-Chien Lee, and Dik-Lun Lee. 2011. Exploiting geographical influence for collaborative point-of-interest recommendation. In *Proceedings of the 34th international ACM SIGIR conference on Research and development in Information Retrieval*. ACM, 325–334.
- [27] Rex Ying, Ruining He, Kaifeng Chen, Pong Eksombatchai, William L Hamilton, and Jure Leskovec. 2018. Graph convolutional neural networks for web-scale recommender systems. In *Proceedings of the 24th ACM SIGKDD International Conference on Knowledge Discovery & Data Mining*. 974–983.
- [28] Quan Yuan, Gao Cong, Zongyang Ma, Aixin Sun, and Nadia Magnenat Thalmann. 2013. Time-aware point-of-interest recommendation. In *Proceedings of the 36th international ACM SIGIR conference on Research and development in information retrieval*. ACM, 363–372.
- [29] Jia-Dong Zhang and Chi-Yin Chow. 2015. GeoSoCa: Exploiting geographical, social and categorical correlations for point-of-interest recommendations. In *Proceedings of the 38th International ACM SIGIR Conference on Research and Development in Information Retrieval*. ACM, 443–452.
- [30] Pengpeng Zhao, Haifeng Zhu, Yanchi Liu, Jiajie Xu, Zhixu Li, Fuzhen Zhuang, Victor S Sheng, and Xiaofang Zhou. 2019. Where to go next: A spatio-temporal gated network for next POI recommendation. In *Proceedings of the AAAI Conference on Artificial Intelligence*, Vol. 33. 5877–5884.
- [31] Shenglin Zhao, Tong Zhao, Irwin King, and Michael R Lyu. 2017. Geo-teaser: Geo-temporal sequential embedding rank for point-of-interest recommendation. In *Proceedings of the 26th international conference on world wide web companion*. International World Wide Web Conferences Steering Committee, 153–162.
- [32] Fan Zhou, Ruiyang Yin, Kunpeng Zhang, Goce Trajcevski, Ting Zhong, and Jin Wu. 2019. Adversarial point-of-interest recommendation. In *The World Wide Web Conference*. 3462–34618.
- [33] Xiao Zhou, Cecilia Mascolo, and Zhongxiang Zhao. 2019. Topic-enhanced memory networks for personalised point-of-interest recommendation. In *Proceedings of the 25th ACM SIGKDD International Conference on Knowledge Discovery & Data Mining*. ACM, 3018–3028.